ACS OMEGA

Open Access

http://pubs.acs.org/journal/acsodf

Article

Lyophilized T Cell Reference Materials with Quantified Proportions of Subtypes

Yinbo Huo, Jiaqi Yang, Yanli Wen, Wen Liang, Qing Tao, Juan Yan, Hui Xu, Lanying Li, Yan Li, Li Xu, Min Ding, Feiyan Gong, and Gang Liu*

Cite This: *ACS Omega* 2024, 9, 48452−48459

Read Online

ACCESS | Metrics & More | Article Recommendations | Supporting Information

ABSTRACT: The accurate quantification of T cell subtypes and their proportions is of great significance in cell-based biomanufacturing, diagnosis, and advanced therapy. The development and application of a cell reference material (RM) provide a solid foundation for reliable and consistent T cell quantification worldwide. However, creating a cell RM that is both accurate and practical remains a challenge. In this study, we have developed a series of T cell RMs with a certified subtype proportion based on traceable accurate quantification and stable long-term preservation. We developed a quantitative flow cytometry method for the ratio of T cell subtypes with improved accuracy by using the calibration of certified reference materials of polystyrene beads. The relative standard deviation (RSD) for the quantification of $CD3^+$, $CD4^+$, and $CD8^+$ subtypes was 0.43%, 0.64%, and 1.31%, respectively. To ensure long-term stability, an innovative lyophilization preservation technique was developed for our T cell RMs. The morphology and surface antigens (CD45, CD3, CD4, and CD8) of T cell RMs were characterized after lyophilization using immunofluorescence, demonstrating their equally good integrity compared with fresh cells. Their stability at 4 °C was demonstrated by continuous monitoring over 12 months. The final value assignment of the RMs was performed through quantification using flow cytometry in different laboratories. One of our RMs has been applied for the calibration of 54 different flow cytometry instruments. The T cell RMs have outstanding potential in the quality control of multiparameter flow cytometry measurements, and we believe they have great application prospects for the establishment and validation of T cell assays.

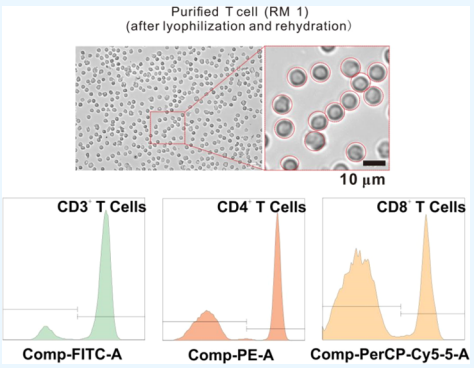

INTRODUCTION

Cell counting[1] is a fundamental measurement in biotechnology. The quantitative analysis of human T cells,[2−4] particularly the ratio of their specific immune phenotypes,[5] plays a vital role in diagnosis[6] and therapy[7,8] across numerous domains. Critical immune phenotypes exhibit different valuable biological functions: $CD8^+$ T cells can exert antitumor effects in vivo, while $CD4^+$ T cells play a crucial role in promoting the function, expansion, and persistence of $CD8^+$ T cells.[9,10] Preclinical studies have suggested that a defined CD4:CD8 ratio could lead to superior antitumor efficacy in CAR-T cell therapy.[11] Therefore, quantification analysis of T cell phenotypes become a widely used tool in clinical diagnosis and cell therapy.[12−14] For example, infection of the human immunodeficiency virus (HIV) leads to a significant reduction in $CD4^+$ T cells,[15] making $CD4^+$ T cell counting a crucial indicator for the determination of treatment for AIDS patients, including the antiretroviral therapy when $CD4^+$ T cell count is below 350 cells/μL or chemoprophylaxis when the $CD4^+$ T cell count is below 200 cells/μL.[16,17] Additionally, the proportions of different T cell subtypes significantly impact the efficacy of immune cell therapies,[18] such as CAR-T cell manufacturing, cell-based pharmacokinetics, and T cell leukemia/lymphoma diagnosis.

Flow cytometry is the most widely used method for the quantification of T cell subtypes.[19] However, the complexity of sample processing and differences in hardware platforms present challenges to achieving consistency and accuracy.[20] Therefore, there is an urgent need for the research of T cell reference materials (RMs) with advanced metrological traceability to improve the reliability of T cell analysis.[21] Fluorescent polystyrene beads have been developed as a high-grade reference material for microparticle counting. The beads typically contain one or more fluorescent dyes with uniform sizes and certified numbers, making them suitable for the calibration of flow cytometry instruments. However, the analysis of beads, which shows different scattering and omits the immunofluorescence labeling process, is not representative

Received: July 31, 2024
Revised: October 4, 2024
Accepted: October 9, 2024
Published: November 25, 2024

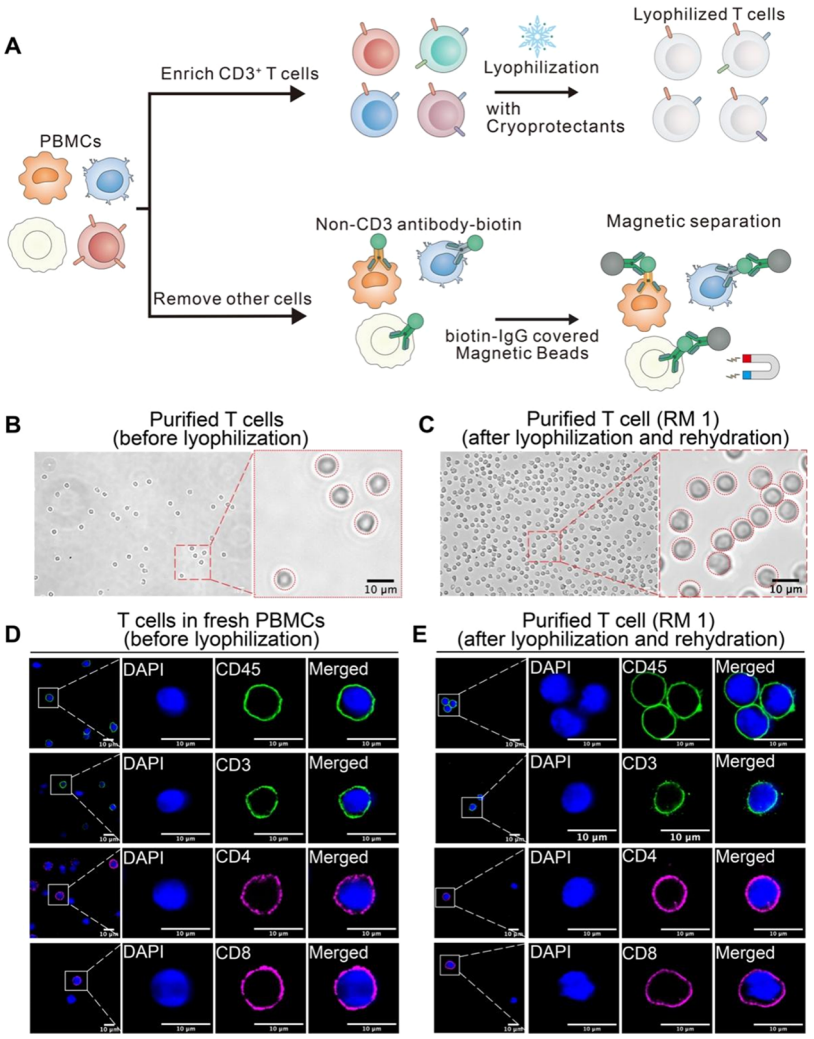

Figure 1. (A) Preparation of T cell RMs including immunospecific enrichment and lyophilization. One-time purification was performed for RM1, and two-time purification was performed for RM2. Optical microscopy images of (B) fresh PBMCs and (C) T cell RM. The red circles indicated T cells. Immunofluorescence images of T cells (D) in fresh PBMCs and (E) in T cell RM. The first column is the entire field of the image, and the second to fourth columns are enlarged images of different channels in the white box. The nucleus was stained with DAPI (blue). T cells were immunostained using specific antibodies. The first line is CD45 (green), the second line is CD3 (green), the third line is CD4 (magenta), and the fourth line is CD8 (magenta). Green: Alexa Fluor 488 conjugated secondary antibody, magenta: Alexa Fluor 647 conjugated secondary antibody. All of the scale bars are 10 μm. RM1 was taken as an example in this figure.

of real cells. Although NIH once developed a standard of CAR/TCR-T cells flow cytometry quality control,[22] its feasibility was quite limited due to the stringent storage conditions in liquid nitrogen. Another critical issue with cell reference materials is the lack of metrological traceability and comparability during cell quantification. In 2017, the National Institute of Standards and Technology (NIST) and the US Food and Drug Administration (FDA) jointly hosted a workshop[23] for cell counting, to address the lack of measurement assurance for cell counting. In general, there is an urgent need to establish real cell reference materials with long-term preservation strategies, accurate quantification, and metrological traceability.

In this study, we developed two T cell RMs (RM1 and RM2) with varying levels of purity and different proportions of the T cell subtype. Initially, the T lymphocytes were purified from peripheral blood mononuclear cells (PBMCs) and lyophilized under optimized experiment conditions. The resulting cell RMs were shown to be uniform and pure, with an excellent intact morphology, even when compared with the fresh cells. We then established a metrologically traceable quantification for cell numbers and portions, using microbeads and RM as internal standards for the calibration of each flow cytometry measurement. The value assignment of the RMs was conducted through coordinated measurements in multiple laboratories, and one of the cell RMs has been widely applied for the calibration of 54 different flow cytometry instruments. We believe these cell RMs will provide valuable support for the quality control and metrological traceability of T cell analysis, contributing to improved consistency across different testing platforms, at different testing times and by different operators.

METHODS AND REAGENTS

Materials and Reagents. Peripheral blood mononuclear cells (PBMCs) from healthy adults were prepared by Hycells (Shanghai) and T cell isolation kit by T cell, Miltenyi Biotec. Antibodies used in the study include APC antihuman CD45 Antibody (Biolegend), fluorescein isothiocyanate (FITC)

https://doi.org/10.1021/acsomega.4c06867
ACS Omega 2024, 9, 48452−48459

antihuman CD3 Antibody (Biolegend), PE antihuman CD4 Antibody (Biolegend), PerCP-Cyanine5.5 antihuman CD8a Antibody (Biolegend), CD45 Monoclonal Antibody (Invitrogen), CD4Monoclonal Antibody (CST), CD3Monoclonal Antibody (Invitrogen), CD8a Monoclonal Antibody (Abcam), Goat anti-Mouse IgG (H + L) Alexa Fluor 488 (Invitrogen), and Donkey anti-Rabbit IgG (H + L) Alexa Fluor 647 (Invitrogen). Phosphate-buffered saline (PBS) (pH 7.2) was from Gibco. Microns Fluorescent Count Particles Reference Material (GBW(E)120142).

T Cell Purification. PBMCs were first incubated with a mixture of biotinylated monoclonal antibodies (anti-CD14, CD15, CD16, CD19, CD34, CD36, CD56, CD123, and CD235a), and then captured by antibiotin-IgG-covered magnetic beads. Finally, these non-T-cells were magnetically separated by using a magnetic field. Finally, most of the $CD3^+$ cells were enriched. This magnetic purification was performed one time for RM1 and two times for RM2, to achieve different levels of purification.

Cell Lyophilization. The purified T lymphocytes were resuspended in a freezing medium containing sucrose in PBS, mixed at 4 °C for 10 min, and then divided into 3 mL glass vials with 1 million cells in each vial. The samples were placed in a vacuum freeze-dryer (Tofflon lyo-0.5) and subjected to 48 h of vacuum lyophilization at −45 °C before being sealed under vacuum.

Rehydration of Lyophilized Samples. The lyophilized T cell RM was brought to room temperature and allowed to stand for at least 10 min before carefully removing the cap of the glass vial. Special attention should be given to the initial low air pressure inside the vial. Then, 0.6 mL of rehydration solution (2% BSA in PBS) was added, followed by gentle mixing and incubation at room temperature for 10 min.

Sample Staining for Flow Cytometric Analysis. Four single-staining samples were prepared by adding a fluorescent labeled antibody (CD45-APC, CD3-FITC, CD4-PE, or CD8-PerCP-Cy5-5, respectively) into the rehydrated cell suspension, while the multistaining was performed by adding all four antibodies together. All samples were incubated in the dark for 1 h after the centrifugation to remove the supernatant at 500*g* for 5 min. The cell pellet was washed with 1 mL of PBS followed by centrifugation again at 500*g* for 5 min. Then, it was resuspended in 1 mL of PBS before being analyzed using a flow cytometer (FACS Canto II, BD). Before quantification, the compensation of the flow cytometer was adjusted using four single-staining samples and one unstained cell sample for a minimal leakage between the four channels. The sample tubes with multistaining were then analyzed, collecting at least 10,000 events each time.

Imaging and Immunofluorescence. Rehydrated T cell RM was incubated with monoclonal antibodies (CD45, CD3, CD4, and CD8) as primary antibodies at room temperature for 1 h to overnight at 4 °C. In the four groups of cells incubated with primary antibodies, species-specific fluorescent secondary antibodies were added and incubated at room temperature in the dark for 1 h. The cells were washed once with 1 mL of PBS and centrifuged to remove the supernatant. The cell pellet from the previous step was resuspended in 50 μL of Antifade Mounting Medium (Beyotime). Immunostained cells were imaged by using a confocal microscope (Leica STELLARIS 8).

RESULTS AND DISCUSSION

T Cell Purification. The development of a cell RM faces critical challenges, including homogeneity, stability, and the realization of specific ratios of cell subtypes. In this section (Figure 1A), we took PBMCs as the starting material and employed a purification process to enrich T cells with the CD3 surface antigen from PBMCs. Through an antigen-specific magnetic separation, most of the other cells expressing nontarget antigens ($CD14^+$, $CD15^+$, $CD16^+$, $CD19^+$, $CD34^+$, $CD36^+$, $CD56^+$, $CD123^+$, and $CD235a^+$) were removed. Two candidate T cell RMs were purified using different levels of magnetic purification: a low-purity T cell RM (RM1) through one-time magnetic separation and a high-purity T cell RM (RM2) through two-time magnetic separation.

The microscopic imaging confirmed the effectiveness of the purification process. In contrast to the fresh T cells (Figure 1B) showing obvious heterogeneity of cell morphology, the purified sample (RM1, as an example) contained predominantly T cells with a consistent cell population (Figure 1C). Furthermore, the components of the prepared cell samples (RM1 and RM2) were also characterized by a flow cytometer. Specifically, 99.9% of all of the remaining cells in both RM1 and RM2 were $CD45^+$ lymphocytes. Among these $CD45^+$ lymphocytes, the proportion of T cells ($CD3^+$) was higher than 89% in RM1 (Figure S1A) and 99% in RM2 (Figure S1B). In summary, two cell samples containing different proportions of T cells were successfully prepared.

Lyophilization. T cells are fragile and prone to breakage, traditionally requiring storage in liquid nitrogen. Lyophilization is a long-term storage method for delicate samples, such as nucleic acids and proteins. However, there is currently a lack of research on lyophilization techniques for T cells. In the absence of a cryoprotectant, T cell rupture occurs after lyophilization-rehydration, limiting the development of T cell RMs. In this study, we optimized the components and concentrations of cryoprotectant for T cells and demonstrated that the cryoprotectant (8% sucrose and 8% trehalose) provides excellent preservation of cell morphology (Figure S2A). Subsequently, we established and optimized a lyophilization for the long-term preservation of the RMs. We researched a cryoprotectant containing sucrose and trehalose to preserve intact cell membranes under harsh freeze-drying conditions. By comparing different concentrations of sucrose and trehalose in our cryoprotectant and assessing the flow cytometry results, we found that (Figure S2B,C) the higher concentration (8% sucrose and 8% trehalose) provided the best protection for the cells, generating the highest MFI of mean fluorescence intensity (MFI) during flow cytometry analysis. In contrast, reduced sucrose and trehalose (2 or 0.5%) led to lower MFI, likely due to damaged cell phenotype or inactivated surface antigens. The microscopic imaging demonstrated the intact cell morphology of our RMs after lyophilization-rehydration (Figure S2D), while many cells were ruptured without this protection (PBS was used instead; Figure S2D).

Immunofluorescence imaging analysis was further conducted to investigate the cell morphology at the subcellular level after lyophilization. Results showed that T cell RM1, rehydrated after lyophilization, exhibited cellular membranes and nuclei that were highly consistent with fresh T cells (Figure 1D). Effective localization of CD45, CD3, CD4, and CD8 on the

https://doi.org/10.1021/acsomega.4c06867
ACS Omega 2024, 9, 48452−48459

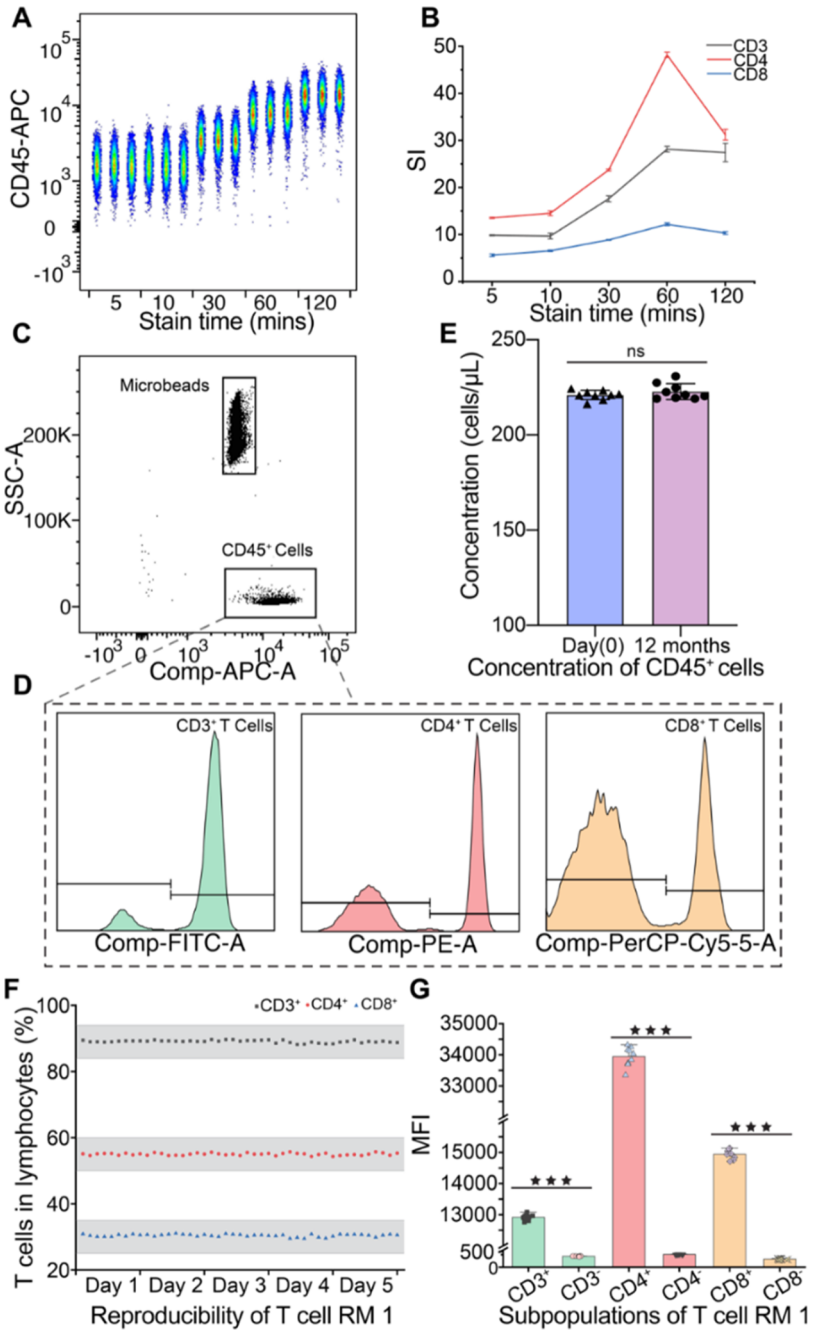

Figure 2. Optimization and investigation of the multiparameter flow cytometry method. (A) Optimization of staining times for CD45, n = 3 independent replicate experiments. (B) Stain index (SI) of CD3, CD4, and CD8 antibodies. (C) Cell counting using calibration of microbeads, and the gating of the $CD45^+$ cells and microbeads. (D) Gating of $CD3^+$, $CD4^+$, and $CD8^+$ cells in the $CD45^+$ cells to obtain the number of events in the defined region. (E) Number of $CD45^+$ cells after one year of storage at 4 °C. Error bars represent standard deviation (SD). P-value >0.05. (F) T cell was subjected to multiparameter flow cytometry analysis for five consecutive days, with nine measurements on each day. The gray area represents the range of ±5% interval of the target value. (G) Statistical of MFI for CD3, CD4, and CD8 in day 5.

cell membrane was also observed (Figure 1E). A similar investigation result was achieved for RM2 (Figure S2E).

These characterization results demonstrate the production of two T cell RMs with specific subtype proportions as well as the successful preservation of the cell morphology after lyophilization.

Quantitative Flow Cytometry for the Value Assignment of T Cell RMs. Establishing flow cytometry for the value assignment of the cell RMs is much more challenging than routinely applied flow cytometry assays due to the higher requirement of accuracy, stability, and precision.[21] This section established a quantification flow cytometry method with solid metrological traceability of cell counting to obtain accurate proportions of subtypes: $CD3^+$, $CD4^+$, and $CD8^+$ in RM1 and $CD4^+$ in RM2.

Initially, antigen staining for flow cytometry was investigated as it significantly affects the discrimination between negative and positive cell populations. Excessive or insufficient staining time can lead to poor discrimination. Staining times for different antigens were studied at intervals of 5, 10, 30, 60, and

https://doi.org/10.1021/acsomega.4c06867
ACS Omega 2024, 9, 48452−48459

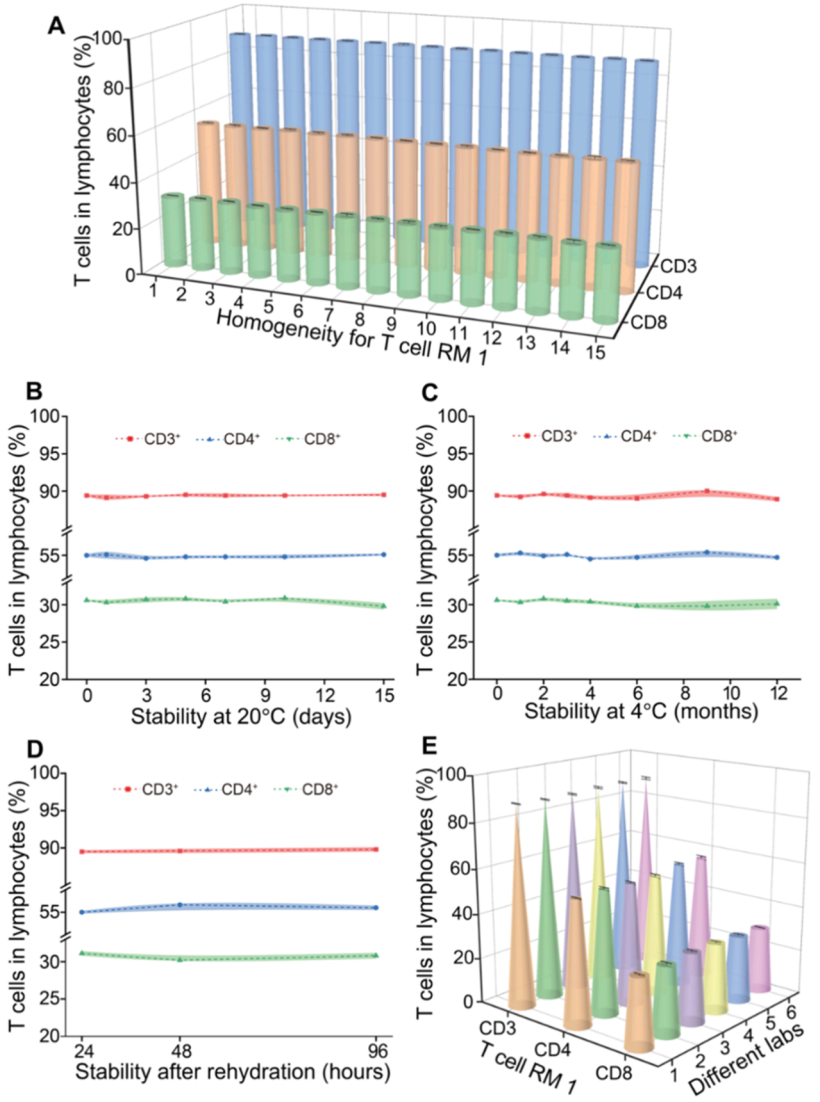

Figure 3. Homogeneity, stability, and cross-laboratory measurements of T cell RM1. (A) Homogeneity investigation. Fifteen randomly selected vials were taken from 200 T cell RM1 samples, and $CD3^+$, $CD4^+$, and $CD8^+$ proportions were measured three times for each sample under the same conditions. (B) Stability of T cell RM1 within 15 days at 20 °C, $n = 3$ independent replicate experiments, error bars represent SD. (C) Stability of T cell RM1 within 12 months at 4 °C, $n = 3$ independent replicate experiments; error bars represent SD. (D) Stability after rehydration of T cell RM1 within 96 h at 4 °C, $n = 3$ independent replicate experiments, error bars represent SD. (E) Measurement results of T cell RM1 from six different laboratories.

120 min, and the fluorescent intensity was compared. As depicted in Figure 2A, the CD45 signal (stained by CD45-APC) increased with longer staining time, reaching its maximum at 120 min.

Similar trends were observed for the positive signals of $CD3^+$, $CD4^+$, and $CD8^+$ cell populations (Figure S3A−C), but some inevitable nonspecific staining of $CD3^-$, $CD4^-$, and $CD8^-$ cells was observed with prolonged staining time. Upon comparison of the stain index (SI), which is the ratio of positive and negative signals, it was determined that a 60 min staining time was optimal for all three antigens ($CD3^+$, $CD4^+$, and $CD8^+$) (Figure 2B).

Second, variation of the sample volume is a critical source of variation for flow cytometry quantification of total cell numbers. To address this, we calibrated our cell counting by using microbeads with a known particle number as an internal standard in flow cytometry.[24,25] As the result showed (Figure 2C), the fluorophores on the microbeads (excitation: 390−630 nm, emission: 500−750 nm) could be detected under the same condition of antibody-stained T cell RM1. The microbeads and cells were dramatically separated into distinct populations in the flow cytometry plots, enabling accurate gating. Subsequently, we obtained the event counts within defined regions containing different subtypes of cells and a known concentration of microbeads. The total number of lymphocytes ($CD45^+$) was measured and calibrated by using eq 1, which was the foundation of the following quantification of the proportions of subtypes: $CD3^+$, $CD4^+$, and $CD8^+$ cells in $CD45^+$ lymphocytes (Figure 2D). The stability of the total number of $CD45^+$ lymphocytes at 4 °C for 12 months was demonstrated (Figure 2E), and its cellular morphology and staining of CD45, CD3, CD4, and CD8 remained consistent with those of fresh T cells (Figure S3D). By introducing the number of microbeads in the RM, which was from absolute counting under a microscope, we established the metrology

https://doi.org/10.1021/acsomega.4c06867
ACS Omega 2024, 9, 48452−48459

traceability of cell counting for the development of our cell RMs.

$$C_{cells} = \frac{N_{cells}}{N_B} \times \frac{N_{BS}}{V} \quad (1)$$

where C_{cells} is the concentration of cells to be measured (cells/μL), N_{cells} is the number of events in defined regions containing cells, N_B is the number of events in defined regions containing microbeads, N_{BS} is the standard particle number in RM of microbeads, and V is the sample volume (μL).

Next, we measured the percentage of three main subtypes: $CD3^+$, $CD4^+$, and $CD8^+$ in total $CD45^+$, using eqs 2−4.

$$P_{CD3} = \frac{C_{CD3}}{C_{CD45}} \times 100\% \quad (2)$$

$$P_{CD4} = \frac{C_{CD4}}{C_{CD45}} \times 100\% \quad (3)$$

$$P_{CD8} = \frac{C_{CD8}}{C_{CD45}} \times 100\% \quad (4)$$

where P_{CD3}, P_{CD4}, and P_{CD8} are the proportions of $CD3^+$, $CD4^+$, and $CD8^+$ cells in T cell RM, respectively.

We further conducted a systematic investigation and optimization of this quantification flow cytometry method. Initially, we assessed the sensitivity by analyzing consecutively diluted cell samples. A specific number of unstained cells were added into our stained cells to achieve a series of cell ratios (stained cells:total cells) of 1:1, 1:10, 1:100, and 1:1000 (Figure S4), which were then quantified by our flow cytometry method. The results showed that the number of detected cells decreased in correlation with the dilution, exhibiting a perfect linear correlation with the dilution factors. Even when the cells were diluted 100 times (1:100), the subtypes of stained cells remained detectable with a low relative standard deviation (RSD) of less than 5%, indicating excellent reliability and precision. Consequently, the detection limit of our method was determined to be 1:100 (Table S1).

Then, we assessed the repeatability and comparability of flow cytometric quantification at different times, which are crucial for RM value assignment. T cell RM1 was analyzed nine times per day over five consecutive days (Figure 2F). The RSD for the quantification of $CD3^+$, $CD4^+$, and $CD8^+$ subtypes was found to be 0.43, 0.64, and 1.31% across five experimental days, respectively (Table S2). Additionally, there was a significant difference in MFI between the positive and negative populations of CD3, CD4, and CD8 (Figure 2G). The flow cytometry results of different cell subtypes indicated that the positive group's MFI was 2 orders of magnitude higher than that of the negative group. In summary, the above results strongly demonstrate the metrology traceability, sensitivity, and repeatability of our quantitative flow cytometry method for the value assignment of T cell RMs.

Quantification and Inspection of Our T Cell RMs. The homogeneity of cell RMs presents more challenges than dissolvable chemical reagents because the dispersibility of cells is low, and vigorous mixing should be avoided for the protection of the cell membrane. Therefore, prior to lyophilization, the cell RMs were separated into 200 vials under very gentle and continuous vortexing. We then investigated the homogeneity between vials by analyzing 15 randomly selected vials. Each sample was measured three times for the proportion of $CD3^+$, $CD4^+$, and $CD8^+$ cells (Figure 3A). Fortunately, the results indicated excellent homogeneity according to single-factor analysis of variance (ANOVA) (Table S3).

The lyophilization step effectively improved the stability of the cell RMs, which is critical for their practical application. We investigated the preservation of lyophilized cell RMs under storage under different conditions by monitoring the proportion of cell subtypes. First, several lyophilized vials of RM1 were stored at ambient temperature (20 °C), and the proportions of $CD3^+$, $CD4^+$, and $CD8^+$ subtypes were measured 7 times over a 15-day period. The results were maintained statistically stable, demonstrating 15-day stability of the cell RMs at 20 °C (Figure 3B and Table S4). Second, a similar investigation of stability was performed under 4 °C, showing longer preservation over 12 months (Figure 3C and Table S5). Third, the stability after rehydration was studied. Some lyophilized T cell RMs were rehydrated by adding PBS containing 2% bovine serum albumin (BSA) and then stored at 4 °C. The cell proportions were measured at 24, 48, and 96 h. The unchanged results proved the stability of rehydrated RMs within 96 h (Figure 3D).

The final measurement for the value assignment was performed across different laboratories involving different operators and facilities. T cell RM1 was measured in six different laboratories for the assignment of average proportions of subtypes (Figure 3E). Excellent consistency was achieved among all 6 results, demonstrated by the small RSD of less than 5% (Table S6). Similarly, four different laboratories participated in the value assignment of T cell RM2, which achieved an accurate average proportion of $CD4^+$ subtypes (Figure S5) with an RSD of 0.97%.

The final uncertainty of the quantification results was evaluated, considering 3 main uncertainty components during the preparation and quantification of the cell RMs: inhomogeneity (u_{hom}), instability (u_{lts}), and characterization (u_{char}) (Table S7). Finally, the results of value assignment for our RMs were: 88.88 ± 8.00% $CD3^+$, 55.11 ± 4.96% $CD4^+$, and 30.35 ± 2.80% for $CD8^+$ in RM1, and 73.37 ± 6.62% $CD4^+$ in RM2.

The Practicability of the Cell RM. The measurement of $CD4^+$ proportion is widely applied in life science and biological medicine, making it the most representative parameter for studying metrology traceability of cell quantification. In this study, we performed the calibration of flow cytometry instruments utilizing RM2, which provides an accurate value of $CD4^+$ proportion. The T cell RM2 was rehydrated and stained with a fluorochrome-conjugated CD4 antibody, followed by flow cytometry analysis in 54 different laboratories, and each participating laboratory performed six measurements of $CD4^+$ cell proportions. All 54 quantification results were collected and analyzed, and the E_n values were calculated to indicate the deviation of each single measurement.

As the results showed (Figure 4), all of the results fell within the range of uncertainty (gray area in Figure 4) of the cell RM2, with 53.7% of the participating laboratories achieving "satisfactory" results ($E_n < 1$). Furthermore, 29.6% of all of the collected E_n values were between 1 and 2, 3.7% between 2 and 3, and the remainder were bigger than 3. Possible interferences for the unsatisfactory results may arise from the human operation, platform differences, and parameter settings. The application of our cell RMs demonstrated their broad prospect in the calibration and validation of cell analysis.

https://doi.org/10.1021/acsomega.4c06867
ACS Omega 2024, 9, 48452−48459

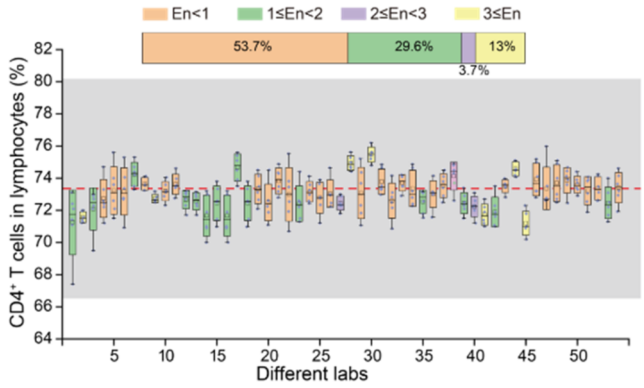

Figure 4. Metrological comparison results using T cell RM2. Each laboratory performed six measurements. Error bars represent SD. The E_n values were calculated based on the results of the proficiency testing. The red line represents 73.37%, which corresponds to the reference value of the T cell RM2. The gray area represents the expanded uncertainty (k = 2) of our cell RM2.

CONCLUSIONS

Flow cytometry is the most important and widely used method for quantitatively analyzing T lymphocyte subtypes in clinical treatment and biomedical research. However, many interference factors present significant challenges to the consistency, accuracy, and comparability of cell measurements. To establish a reliable metrological standard for cell quantification, we developed two T cell RMs with high homogeneity and accurate proportions of the subtypes. Long-term preservation was achieved using a lyophilization treatment, and the integrity of the cell membrane and the accessibility for antibody staining was demonstrated to be as good as fresh cells.

We developed a quantitative flow cytometry with excellent stability, repeatability, and precision. Most importantly, the metrological traceability for each cell counting was established through the calibration of a reference material of microbeads. The value assignment for the T cell RMs was performed in several different laboratories. The stability of T cell RM was well proved by continuous monitoring over one year of storage at 4 °C, which is critical for their practicability. Finally, we applied one of our RM for a wide range of calibration of flow cytometry instruments. The comparison of results revealed the challenges of consistency among different platforms because only 53.7% of the participating laboratories reached satisfactory results (E_n < 1); however, on the other side, all of the deviations of PT results are smaller than the uncertainty, demonstrating the reasonability of our uncertainty evaluation.

In summary, our T cell RMs provided an accurate benchmark for T cell flow cytometry measurements, serving as a quality control of flow cytometry methods and instrument performance evaluation.

ASSOCIATED CONTENT

Supporting Information

The Supporting Information is available free of charge at https://pubs.acs.org/doi/10.1021/acsomega.4c06867.

Characterization of T cell RM2, comparison of cryoprotectants, study of antibody staining time, assessment of sensitivity, data of the value assignment, assessment of homogeneity and stability, and evaluation of uncertainty (PDF)

AUTHOR INFORMATION

Corresponding Author

Gang Liu − *Key Laboratory of Bioanalysis and Metrology for State Market Regulation, Shanghai Institute of Measurement and Testing Technology, Shanghai 201203, China;* orcid.org/0000-0003-3779-7212; Phone: +862138839800; Email: liug@simt.com.cn

Authors

Yinbo Huo − *Key Laboratory of Bioanalysis and Metrology for State Market Regulation, Shanghai Institute of Measurement and Testing Technology, Shanghai 201203, China*

Jiaqi Yang − *College of Food Science & Technology Shanghai Ocean University, Shanghai 201306, China*

Yanli Wen − *Key Laboratory of Bioanalysis and Metrology for State Market Regulation, Shanghai Institute of Measurement and Testing Technology, Shanghai 201203, China*

Wen Liang − *Key Laboratory of Bioanalysis and Metrology for State Market Regulation, Shanghai Institute of Measurement and Testing Technology, Shanghai 201203, China*

Qing Tao − *Key Laboratory of Bioanalysis and Metrology for State Market Regulation, Shanghai Institute of Measurement and Testing Technology, Shanghai 201203, China*

Juan Yan − *College of Food Science & Technology Shanghai Ocean University, Shanghai 201306, China;* orcid.org/0000-0003-4529-2046

Hui Xu − *School of Intelligent Manufacturing, Huzhou College, Huzhou 313000, China*

Lanying Li − *Key Laboratory of Bioanalysis and Metrology for State Market Regulation, Shanghai Institute of Measurement and Testing Technology, Shanghai 201203, China*

Yan Li − *Key Laboratory of Bioanalysis and Metrology for State Market Regulation, Shanghai Institute of Measurement and Testing Technology, Shanghai 201203, China*

Li Xu − *Key Laboratory of Bioanalysis and Metrology for State Market Regulation, Shanghai Institute of Measurement and Testing Technology, Shanghai 201203, China*

Min Ding − *Key Laboratory of Bioanalysis and Metrology for State Market Regulation, Shanghai Institute of Measurement and Testing Technology, Shanghai 201203, China*

Feiyan Gong − *Key Laboratory of Bioanalysis and Metrology for State Market Regulation, Shanghai Institute of Measurement and Testing Technology, Shanghai 201203, China*

Complete contact information is available at: https://pubs.acs.org/10.1021/acsomega.4c06867

Author Contributions

Y.H. and J.Y. performed the cell preparation and flow cytometry. Y.W. and W.L. studied the lyophilization. Q.T. carried out cell characterization. J.Y supervised the research. L.L. performed the data analysis. Y.L. and L.X. carried out the calibration. M.D. investigated the stability. F.G. studied the homogeneity. G.L. interpreted data and wrote the paper.

Notes

The authors declare no competing financial interest.

ACKNOWLEDGMENTS

This work was financially supported by National Administration for Market Regulation Technology Support Special Project (2023YJ01), the National Natural Science Foundation of China (No. 22074093), Shanghai Commission of Science

https://doi.org/10.1021/acsomega.4c06867
ACS Omega 2024, 9, 48452−48459

and Technology (No. 23002400200), and Shanghai Market Supervision and Administration Bureau (2022-13).

REFERENCES

(1) Tang, W.; Tang, D.; Ni, Z.; Xiang, N.; Yi, H. Microfluidic Impedance Cytometer with Inertial Focusing and Liquid Electrodes for High-Throughput Cell Counting and Discrimination. *Anal. Chem.* **2017**, *89* (5), 3154−3161.
(2) Walsh, A. J.; Mueller, K. P.; Tweed, K.; Jones, I.; Walsh, C. M.; Piscopo, N. J.; Niemi, N. M.; Pagliarini, D. J.; Saha, K.; Skala, M. C. Classification of T-cell activation via autofluorescence lifetime imaging. *Nat. Biomed. Eng.* **2021**, *5* (1), 77−88.
(3) Jaeger, N.; Gamini, R.; Cella, M.; Schettini, J. L.; Bugatti, M.; Zhao, S. R.; Rosadini, C. V.; Esaulova, E.; Di Luccia, B.; Kinnett, B.; et al. Single-cell analyses of Crohn's disease tissues reveal intestinal intraepithelial T cells heterogeneity and altered subset distributions. *Nat. Commun.* **2021**, *12* (1), No. 1921, DOI: 10.1038/s41467-021-22164-6.
(4) Yazdani, S.; Seitz, C.; Cui, C.; Lovik, A.; Pan, L.; Piehl, F.; Pawitan, Y.; Kläppe, U.; Press, R.; Samuelsson, K.; et al. T cell responses at diagnosis of amyotrophic lateral sclerosis predict disease progression. *Nat. Commun.* **2022**, *13* (1), No. 6733, DOI: 10.1038/s41467-022-34526-9.
(5) Shinoda, K.; Lia, R.; Rezk, A.; Mexhitaj, I.; Patterson, K. R.; Kakara, M.; Zuroff, L.; Bennett, J. L.; von Büdingen, H. C.; Carruthers, R.; et al. Differential effects of anti-CD20 therapy on CD4 and CD8 T cells and implication of CD20-expressing CD8 T cells in MS disease activity. *Proc. Natl. Acad. Sci. U.S.A.* **2023**, *120* (3), No. e2207291120.
(6) Mahalingam, S. S.; Jayaraman, S.; Bhaskaran, N.; Schneider, E.; Faddoul, F.; Paes da Silva, A.; da Silva, A. P.; Lederman, M. M.; Asaad, R.; Adkins-Travis, K.; Shriver, L. P. Polyamine metabolism impacts T cell dysfunction in the oral mucosa of people living with HIV. *Nat. Commun.* **2023**, *14* (1), No. 399, DOI: 10.1038/s41467-023-36163-2.
(7) Saberzadeh-Ardestani, B.; Graham, R. P.; McMahon, S.; Ahanonu, E.; Shi, Q.; Williams, C.; Hubbard, A.; Zhang, W. J.; Muranyi, A.; Yan, D. Y.; et al. Immune Marker Spatial Distribution and Clinical Outcome after PD-1 Blockade in Mismatch Repair-deficient, Advanced Colorectal Carcinomas. *Clin. Cancer Res.* **2023**, *29* (20), 4268−4277.
(8) Peng, S. H.; Hu, P.; Xiao, Y. T.; Lu, W. Q.; Guo, D. D.; Hu, S. X.; Xie, J. Y.; Wang, M. N.; Yu, W. W.; Yang, J. J.; et al. Single-Cell Analysis Reveals EP4 as a Target for Restoring T-Cell Infiltration and Sensitizing Prostate Cancer to Immunotherapy. *Clin. Cancer Res.* **2022**, *28* (3), 552−567.
(9) Barberis, M.; Rojas López, A. T cell phenotype switching in autoimmune disorders: Clinical significance of targeting metabolism. *Clin. Transl. Med.* **2022**, *12* (7), No. e898.
(10) Wik, J. A.; Skålhegg, B. S. T. Cell Metabolism in Infection. *Front. Immunol.* **2022**, *13*, No. 840610.
(11) Golubovskaya, V.; Wu, L. Different Subsets of T Cells, Memory, Effector Functions, and CAR-T Immunotherapy. *Cancers* **2016**, *8* (3), No. 36, DOI: 10.3390/cancers8030036.
(12) Kumar, B. V.; Connors, T. J.; Farber, D. L. Human T Cell Development, Localization, and Function throughout Life. *Immunity* **2018**, *48* (2), 202−213.
(13) Thastrup, M.; Marquart, H. V.; Levinsen, M.; Modvig, S.; Abrahamsson, J.; Albertsen, B. K.; Frost, B. M.; Harila-Saari, A.; Pesola, J.; Ulvmoen, A.; et al. Flow cytometric analysis of cerebrospinal fluid improves detection of leukaemic blasts in infants with acute lymphoblastic leukaemia. *Br. J. Haematol.* **2021**, *195* (1), 119−122.
(14) Garcia, J.; Daniels, J.; Lee, Y.; Zhu, I.; Cheng, K.; Liu, Q.; Goodman, D.; Burnett, C.; Law, C.; Thienpont, C.; et al. Naturally occurring T cell mutations enhance engineered T cell therapies. *Nature* **2024**, *626* (7999), 626−634.
(15) Detels, R.; Muñoz, A.; McFarlane, G.; Kingsley, L. A.; Margolick, J. B.; Giorgi, J.; Schrager, L. K.; Phair, J. P. Effectiveness of potent antiretroviral therapy on time to AIDS and death in men with known HIV infection duration. Multicenter AIDS Cohort Study Investigators. *Jama* **1998**, *280* (17), 1497−1503.
(16) Kaplan, J. E.; Benson, C.; Holmes, K. K.; Brooks, J. T.; Pau, A.; Masur, H. Guidelines for prevention and treatment of opportunistic infections in HIV-infected adults and adolescents: recommendations from CDC, the National Institutes of Health, and the HIV Medicine Association of the Infectious Diseases Society of America. *MMWR Recomm. Rep.* **2009**, *58* (4), 1−207.
(17) Mandy, F. F.; Nicholson, J. K.; McDougal, J. S. Guidelines for performing single-platform absolute CD4+ T-cell determinations with CD45 gating for persons infected with human immunodeficiency virus. Centers for Disease Control and Prevention. *MMWR Recomm. Rep.* **2003**, *52* (2), 1−13.
(18) Schillebeeckx, I.; Earls, J.; Flanagan, K. C.; Hiken, J.; Bode, A.; Armstrong, J. R.; Messina, D. N.; Adkins, D.; Ley, J.; Alborelli, I.; et al. T cell subtype profiling measures exhaustion and predicts anti-PD-1 response. *Sci. Rep.* **2022**, *12* (1), No. 1342.
(19) Lambert, C.; Yanikkaya Demirel, G.; Keller, T.; Preijers, F.; Psarra, K.; Schiemann, M.; Özçürümez, M.; Sack, U. Flow Cytometric Analyses of Lymphocyte Markers in Immune Oncology: A Comprehensive Guidance for Validation Practice According to Laws and Standards. *Front. Immunol.* **2020**, *11*, 2169.
(20) Robert, S.; Poncelet, P.; Lacroix, R.; Arnaud, L.; Giraudo, L.; Hauchard, A.; Sampol, J.; Dignat-George, F. Standardization of platelet-derived microparticle counting using calibrated beads and a Cytomics FC500 routine flow cytometer: a first step towards multicenter studies? *J. Thromb. Haemostasis* **2009**, *7* (1), 190−197.
(21) Miller, W. G.; Myers, G.; Cobbaert, C. M.; Young, I. S.; Theodorsson, E.; Wielgosz, R. I.; Westwood, S.; Maniguet, S.; Gillery, P. Overcoming challenges regarding reference materials and regulations that influence global standardization of medical laboratory testing results. *Clin. Chem. Lab. Med.* **2023**, *61* (1), 48−54.
(22) Cai, Y.; Prochazkova, M.; Jiang, C.; Song, H. W.; Jin, J.; Moses, L.; Gkitsas, N.; Somerville, R. P.; Highfill, S. L.; Panch, S.; et al. Establishment and validation of in-house cryopreserved CAR/TCR-T cell flow cytometry quality control. *J. Transl. Med.* **2021**, *19* (1), 523.
(23) Lin-Gibson, S.; Sarkar, S.; Elliott, J. T. Summary of the National Institute of Standards and Technology and US Food And Drug Administration cell counting workshop: Sharing practices in cell counting measurements. *Cytotherapy* **2018**, *20* (6), 785−795.
(24) DeRose, P. C.; Benkstein, K. D.; Elsheikh, E. B.; Gaigalas, A. K.; Lehman, S. E.; Ripple, D. C.; Tian, L.; Vreeland, W. N.; Welch, E. J.; York, A. W.; et al. Number Concentration Measurements of Polystyrene Submicrometer Particles. *Nanomaterials* **2022**, *12* (18), 3118.
(25) Sun, L.; Wu, H.; Pan, B.; Wang, B.; Guo, W. Evaluation and validation of a novel 10-color flow cytometer. *J. Clin. Lab. Anal.* **2021**, *35* (11), No. e23834.

https://doi.org/10.1021/acsomega.4c06867
ACS Omega 2024, 9, 48452−48459